

Computational Model for Compressible Two-Phase Flow in Deformed Porous Medium

Evgeniy Romenski[1(✉)], Galina Reshetova[1,2], and Ilya Peshkov[1,3]

[1] Sobolev Institute of Mathematics SB RAS, Novosibirsk 630090, Russia
evrom@math.nsc.ru
[2] Institute of Computational Mathematics and Mathematical Geophysics SB RAS, Novosibirsk 630090, Russia
kgv@nmsf.sscc.ru
[3] Department of Civil, Environmental and Mechanical Engineering, University of Trento, Via Mesiano 77, Trento, Italy
ilya.peshkov@unitn.it

Abstract. A new three-phase model of compressible two-fluid flows in a deformed porous medium is presented. The derivation of the model is based on the application of the Symmetric Hyperbolic Thermodynamically Compatible (SHTC) systems theory to three-phase solid-fluid mixture. The resulting governing equations are hyperbolic and satisfy the laws of irreversible thermodynamics - conservation of energy and growth of entropy. Due to these properties, the formulated model is well suited for the straightforward application of advanced high accuracy numerical methods applicable to the solution of hyperbolic systems, and ensures the reliability of the numerically obtained solutions. On the basis of the formulated nonlinear model, the governing equations for the propagation of small-amplitude waves are obtained, allowing the use of an efficient finite-difference scheme on staggered grids for their numerical solution. Some numerical examples are presented showing the features of wave propagation in a porous medium saturated with a mixture of liquid and gas with their different ratios.

Keywords: Poroelasticity · Three-phase flow · Symmetric hyperbolic thermodynamically compatible model · Wave propagation

The work is supported by Mathematical Center in Akademgorodok, the agreement with Ministry of Science and High Education of the Russian Federation number 075-15-2019-1613. I.P. also acknowledge funding from the Italian Ministry of Education, University and Research (MIUR) under the Departments of Excellence Initiative 2018–2022 attributed to DICAM of the University of Trento (grant L. 232/2016), as well as financial support from the University of Trento under the *Strategic Initiative Modeling and Simulation*. I.P. has further received funding from the University of Trento via the *UniTN Starting Grant initiative*.

© Springer Nature Switzerland AG 2021
O. Gervasi et al. (Eds.): ICCSA 2021, LNCS 12949, pp. 224–236, 2021.
https://doi.org/10.1007/978-3-030-86653-2_16

1 Introduction

Studies on modeling of saturated porous media began in the middle of the last century in the works of Biot [1,2], and then Biot's model of the propagation of elastic waves in porous media and some of its modifications were used in the study of many scientific problems and seismic applications (see, for example [3,4] and references therein). Biot-type models are limited to considering small elastic deformations, while studying modern industrial problems requires new advanced models that take into account finite deformations and complex rheology of saturating fluids.

Multiphase flow approach can be successfully used to design new models of saturated porous media. In papers by Wilmanski [5,6] it is shown that Biot's theory can be interpreted within a two-phase liquid-solid mixture model with some degree of accuracy. In the present paper we formulate a new computational model for compressible two-phase flow in deformed porous medium and its application to simulations of small amplitude wavefields. The derivation of the full nonlinear model generalizes the model of porous medium saturated with single compressible fluid described in [7,8], which is in turn generalizes the so-called unified model of continuum [9,10] and is based on the theory of the Symmetric Hyperbolic Thermodynamically Compatible (SHTC) systems. Two mechanisms of phase interaction are taken into account: phase pressures relaxation to the common value and interfacial friction. The governing equations of the model are hyperbolic, and their solutions satisfy the laws of irreversible thermodynamics.

On the basis of the formulated nonlinear equations under assumption of instantaneous phase pressures relaxation, a model for small amplitude wave propagation in a stationary unstressed state is derived. It turns out that two compression waves are presented in the model, fast and slow, as in the theory of a porous medium saturated with a single fluid. The solution of a series of test problems in which the saturating fluid is a mixture of liquid and gas demonstrates the strong dependence of the waves behavior on the ratio of the volume fractions of fluids.

The presented model and its generalization for the case of arbitrary number of saturating fluids can be used to numerical modeling of compressible fluids flow in deformed porous media at different scales from slow filtration-type to high-rate deformations flows.

2 Three-Phase Thermodynamically Compatible Model for Compressible Two-Phase Flow in Deformed Porous Medium

2.1 Master System for Derivation of the Model

The derivation of the model is based on the synthesis of a unified continuum model [9] and a compressible multiphase flow model [11], as a result of which a three-phase model of a mixture of two fluid phases and a solid phase can be

obtained. The presented in this paper model generalizes the two-phase SHTC solid-fluid model for fluid saturated porous medium presented in [7,8] and can be designed for an arbitrary number of fluid mixture constituents in a similar way. Let us consider a three-phase continuum with phase volume fractions $\alpha_1, \alpha_2, \alpha_3$ satisfying the saturation constraint $\alpha_1 + \alpha_2 + \alpha_3 = 1$. Further we assume that phases with number $1, 2$ are fluids and the solid phase is numbered as 3. Thus, the porosity is defined as $\phi = \alpha_1 + \alpha_2 = 1 - \alpha_3$. The generalization of the two-phase solid-fluid flow master system presented in [7] for the three-phase case reads as

$$
\begin{aligned}
&\frac{\partial \rho v^i}{\partial t} + \frac{\partial (\rho v^i v^k + \rho^2 E_\rho \delta_{ik} + w_n^i E_{w_n^k} + \rho A_{ki} E_{A_{kj}})}{\partial x_k} = 0,\\
&\frac{\partial \rho}{\partial t} + \frac{\partial \rho v^k}{\partial x_k} = 0,\\
&\frac{\partial A_{ik}}{\partial t} + \frac{\partial A_{im} v^m}{\partial x_k} + v^j \left(\frac{\partial A_{ik}}{\partial x_j} - \frac{\partial A_{ij}}{\partial x_k} \right) = -\Psi_{ik},\\
&\frac{\partial \rho c_a}{\partial t} + \frac{\partial (\rho c_a v^k + \rho E_{w_a^k})}{\partial x_k} = 0, \qquad a = 1, 2,\\
&\frac{\partial w_a^k}{\partial t} + \frac{\partial (w_a^l v^l + E_{c_a})}{\partial x_k} + v^l \left(\frac{\partial w_a^k}{\partial x_l} - \frac{\partial w_a^l}{\partial x_k} \right) = -\Lambda_a^k, \quad a = 1, 2\\
&\frac{\partial \rho \alpha_a}{\partial t} + \frac{\partial \rho \alpha_a v^k}{\partial x_k} = -\Phi_a, \quad a = 1, 2,\\
&\frac{\partial \rho s}{\partial t} + \frac{\partial \rho s v^k}{\partial x_k} = Q.
\end{aligned}
\tag{1}
$$

Here, $\rho = \alpha_1 \rho_1 + \alpha_2 \rho_2 + \alpha_3 \rho_3$ is the total density of the mixture, ρ_1, ρ_2, ρ_3 are the mass densities of fluids and solid, $c_a = \alpha_a \rho_a / \rho$, $(a = 1, 2)$ are mass fractions of fluids ($c_3 = 1 - c_1 - c_2 = \alpha_3 \rho_3 / \rho$ is the solid phase mass fraction), $v^i = c_1 v_1^i + c_2 v_2^i + c_3 v_3^i$ is the mixture velocity, v_1^i, v_2^i are velocities of fluids and v_3^i is the solid phase velocities, $w_a^k = v_a^i - v_3^i$, $a = 1, 2$ are the relative velocity of motion of fluids phase with respect to solid phase, s is the entropy of the mixture, A_{ik} is the distortion matrix, characterizing the elastic deformation of the mixture. Summation over repeated tensor indices $i, j, k, \ldots = 1, 2, 3$ is implied. No summation over repeated phase indices $a, b, c = 1, 2, 3$ is implied unless it is state otherwise via the summation symbol.

The first and second equations of system (1) are the total momentum and total mass conservation laws for the mixture. The third equation controls the evolution of the mixture distortion matrix (in the case of elastic deformation of a pure solid, this is the inverse deformation gradient). The fourth equation is mass conservation law for fluids. The fifth one is the equation for the velocity of the movement of each fluid relative to the solid phase. The six equation governs the fluid volume fractions and the last one is the mixture entropy balance law. The

source term in the latter equation provides the mixture entropy growing as the second law of thermodynamics requires due to the special choice of source terms in (1) for dissipative processes. The dissipative source terms are defined by the thermodynamic forces computed from the given generalized energy E and they are presented below.

To close equations (1) one needs to define a generalized energy E as a function of state variables $\rho, A_{ik}, c_1, c_2, \alpha_1, \alpha_2, w_1^k, w_2^k, s$. Then, thermodynamic forces are computed via derivatives E_ρ, $E_{A_{kj}}$, E_{w_k}, E_{c_1}, E_s as

$$\Phi_a = \rho \sum_{b=1}^{2} \phi_{ab} E_{\alpha_b}, \quad \Lambda_a^k = \sum_{b=1}^{2} \lambda_{ab} E_{w_b^k}, \quad \Psi_{ik} = \frac{1}{\theta} E_{A_{ik}}, \quad a = 1, 2. \tag{2}$$

Here, Φ_a is responsible for the phase pressures relaxation to a common value, Λ_a^k simulates the interfacial friction between phases and Ψ_{ik} is the rate of inelastic deformation of the entire mixture. The entropy production reads as

$$Q = \frac{\rho}{E_s} \sum_{a=1}^{2} \sum_{b=1}^{2} \phi_{ab} E_{\alpha_a} E_{\alpha_b} + \frac{\rho}{E_s} \sum_{a=1}^{2} \sum_{b=1}^{2} \lambda_{ab} E_{w_a^k} E_{w_b^k} + \frac{\rho}{\theta E_s} E_{A_{ik}} E_{A_{ik}} \geq 0, \tag{3}$$

that means that the second law of thermodynamics is satisfied if matrices λ_{ab} and ϕ_{ab} are positive definite.

Pressure p, shear stress tensor σ_{ij} and temperature T are also computed via generalized energy as:

$$p = \rho^2 E_\rho, \quad \sigma_{ij} = -\rho A_{ki} E_{A_{kj}}, \quad T = E_s. \tag{4}$$

The solutions of system (1) also satisfy the first law of thermodynamics – the energy conservation law, which reads as

$$\frac{\partial \rho(E + v^i v^i/2)}{\partial t} + \frac{\partial (\rho v^k (E + v^i v^i/2) + \Pi_k)}{\partial x_k} = 0, \tag{5}$$

where $\Pi_k = v^k p - v^i \sigma_{ik} + \sum\limits_{a=1}^{2} \rho v^l w_a^l E_{w_a^k} + \sum\limits_{a=1}^{2} \rho E_{c_a} E_{w_a^k}$ is the energy flux.

Assume that kinetic coefficients satisfy Onzager's principle, that means that matrices ϕ_{ab}, λ_{ab} are symmetric and can be a functions of state variables. Parameter θ characterizes the rate of inelastic deformation of the mixture and can also be a function of state variables.

The presented equations (1) by construction belong to the class of SHTC systems, that means that they satisfy thermodynamic laws (as we just noted above) and can be transformed into a symmetric form, which is hyperbolic in the sense of Friedrichs, if the generalized energy is a convex function.

For our goals we define the generalized energy E as a sum of the kinematic energy of the relative motion E_1, the energy of volumetric deformation E_2, and the energy of shear deformation E_3:

$$E = E_1(c_1, c_2, w_1, w_2) + E_2(\alpha_1, \alpha_2, c_1, c_2, \rho, s) + E_3(c_1, c_2, \rho, s, A). \tag{6}$$

The kinematic energy of relative motion is defined as

$$E_1 = \frac{1}{2}\sum_{a=1}^{2} c_a w_a^i w_a^i - \frac{1}{2}(\sum_{a=1}^{2} c_a w_a^i)^2. \tag{7}$$

Note that this choice is unique and caused by the fact that with the use of definition of the mixture and relative velocities one can obtain the following identity

$$\rho\left(\frac{v^i v^i}{2} + E_1\right) = \alpha_1\rho_1\frac{v_1^i v_1^i}{2} + \alpha_2\rho_2\frac{v_2^i v_2^i}{2} + \alpha_3\rho_3\frac{v_3^i v_3^i}{2}, \tag{8}$$

and this is exactly the total kinetic energy of the mixture. The energy of volumetric deformation is supposed to be additive:

$$\rho E_2(\alpha_1, \alpha_2, c_1, c_2, \rho, s) = \alpha_1\rho_1 e_1(\rho_1, s) + \alpha_2\rho_2 e_2(\rho_2, s) + \alpha_3\rho_3 e_3(\rho_3, s), \tag{9}$$

with $e_a(\rho_a, s)$, $a = 1, 2, 3$ being the phase internal energies. The latter is equivalent to

$$E_2(\alpha_1, \alpha_2, c_1, c_2, \rho, s) = c_1 e_1\left(\frac{\rho c_1}{\alpha_1}, s\right) + c_2 e_2\left(\frac{\rho c_2}{\alpha_2}, s\right) + c_3 e_3\left(\frac{\rho c_3}{\alpha_3}, s\right). \tag{10}$$

The shear energy E_3 depends on the distortion of the entire mixture and is defined as

$$E_3 = \frac{1}{8}c_{s,M}^2\left(tr(\mathbf{g}^2) - 3\right), \tag{11}$$

where $c_{s,M}$ is the shear sound velocity of the mixture which is determined below, and $\mathbf{g}$ is the normalized Finger (metric) strain tensor: $\mathbf{g} = \mathbf{G}/(\det\mathbf{G})^{1/3}$, $\mathbf{G} = \mathbf{A}^T\mathbf{A}$.

The shear velocity of the mixture should depend on the phase ratio and we define it by the simple mixture rule

$$c_{s,M}^2 = c_1 c_{s,1}^2 + c_2 c_{s,2}^2 + c_3 c_{s,3}^2, \tag{12}$$

where $c_{s,a}$, $a = 1, 2, 3$ are phase shear sound velocities connected with phase shear moduli μ_a by relation $c_{s,a}^2 = \mu_a/\rho_a$. The fluid shear sound velocities can be finite (non-zero), if we consider the viscous hyperbolic model for fluid as it is done in [7]. In this paper, the influence of the viscosity of saturating fluids on the flow is not taken into account, and we assume that the viscosity affects only the interfacial friction. That is why we take the velocities of shear sound waves of both fluids zero and the mixture shear sound velocity reads as

$$c_{s,M}^2 = c_3 c_{s,3}^2 = (1 - c_1 - c_2)c_{s,3}^2. \tag{13}$$

Using the definition of the generalized energy given above and relationships between mixture and phase parameters, we can compute all thermodynamic functions E_α, E_ρ, $E_{A_{kj}}$, $E_{w_a^k}$, E_{c_a}, $p = \rho^2 E_\rho$, $\sigma_{ij} = -\rho A_{ki} E_{A_{kj}}$, $T = E_s$:

$$E_{\alpha_a} = \frac{p_3 - p_a}{\rho}\ (a = 1, 2), \quad p = \rho^2 E_\rho = \alpha_1 p_1 + \alpha_2 p_2 + \alpha_3 p_3,$$

$$\frac{\partial E}{\partial \mathbf{A}} = \frac{c_{s,M}^2}{2}\mathbf{A}^{-T}\left(\mathbf{g}^2 - \frac{tr(\mathbf{g}^2)}{3}\mathbf{I}\right), \quad \sigma_{ij} = -\frac{\rho c_{s,M}^2}{2}\left(g_{ik}g_{kj} - \frac{1}{3}g_{mn}g_{nm}\delta_{ij}\right),$$

$$E_{w_a^i} = c_a w_a^i - c_a(c_1 w_1^i + c_2 w_2^i) = -c_a(v^i - v_a^i), \tag{14}$$

$$E_{c_a} = e_a + \frac{p_a}{\rho_a} - e_3 - \frac{p_3}{\rho_3} - \frac{c_{s,3}^2}{c_{s,M}^2}E_3 + \frac{1}{2}w_a^i(w_a^i - c_1 w_1^i - c_2 w_2^i),\ (a = 1, 2),$$

$$E_s = T = c_1\frac{\partial e_1}{\partial s} + c_2\frac{\partial e_2}{\partial s} + c_3\frac{\partial e_3}{\partial s}.$$

For the closure of the model it is also necessary to define coefficients in the source terms $\Phi_a, \Lambda_a^k, \Psi_{ik}$. The choice of these coefficients may depend on the types of saturating fluids and solid skeleton.

The presented above PDE system along with the closure relations can be used for numerical modeling of compressible two-phase mixture flow in the deformed porous medium in different regimes of flow, from the slow-filtration type flow to high-rate deformation of saturated porous medium. Int the next section we derive the simplified version of the presented model applicable to wavefields simulation.

3 Small Amplitude Wave Propagation in the Porous Medium Saturated by Two-Fluid Mixture

The derivation of the governing PDE system for the small amplitude wave propagation in an immovable medium can be done in a standard linearization procedure, as it is described in [7] for the simpler model of the elastic porous medium saturated with a single fluid. First of all, we assume that the temperature variations in the considered processes are small and, thus, the entropy can be excluded from the set of state variables. This means that the entropy balance law can also be neglected.

Consider an unstressed medium and denote the state variables of this medium by the symbol "0". Assume that the initial value of the fluid volume fractions α_1^0, α_2^0 and solid volume fraction α_3^0 ($\alpha_1^0 + \alpha_2^0 + \alpha_3^0 = 1$) are known. The immovability of the medium means that phase velocities are equal to zero $v_{10}^i = 0, v_{20}^i = 0, v_{30}^i = 0$. In the unstressed state, the pressure and shear stress of the mixture are also equal to zero, that means that $p_1^0 = p_2^0 = p_3^0 = p^0 = 0$, $\sigma_{ik}^0 = 0$. This unstressed state corresponds to reference phase density values $\rho_{10}, \rho_{20}, \rho_{30}$ and to the distortion $A_{ij}^0 = \delta_{ij}$.

We assume that the phase pressure relaxation is instantaneous due to small pore scale. This means that we should replace in the model the evolution equations for the phase volume fractions with the algebraic equations $p_1 = p_2 = p_2 = p$. Then we replace the small variations of distortion by the small deformation tensor and after linearization of stress-strain relations we

arrive to Hook's law connecting shear stress and shear strain. Details of this transformation can be found in [7]. As a result, denoting small variations of the velocity of the mixture V^i, phase relative velocities W_1^i, W_2^i, pressure P and shear stress tensor Σ_{ik}, we arrive to the following system for small amplitude wave propagation in a porous medium saturated with two -fluid compressible mixture

$$\rho_0 \frac{\partial V^i}{\partial t} + \frac{\partial P}{\partial x_i} - \frac{\partial \Sigma_{ik}}{\partial x_k} = 0, \tag{15a}$$

$$\frac{\partial W_1^i}{\partial t} + \left(\frac{1}{\rho_1^0} - \frac{1}{\rho_3^0}\right)\frac{\partial P}{\partial x_i} = -\Lambda_1^i = -\lambda_{11} c_1^0 (V^i - V_1^i) - \lambda_{12} c_2^0 (V^i - V_2^i), \tag{15b}$$

$$\frac{\partial W_2^i}{\partial t} + \left(\frac{1}{\rho_2^0} - \frac{1}{\rho_3^0}\right)\frac{\partial P}{\partial x_i} = -\Lambda_2^i = -\lambda_{21} c_1^0 (V^i - V_1^i) - \lambda_{22} c_2^0 (V^i - V_2^i), \tag{15c}$$

$$\frac{\partial P}{\partial t} + K\frac{\partial V^k}{\partial x_k} + K_1'\frac{\partial W_1^k}{\partial x_k} + K_2'\frac{\partial W_2^k}{\partial x_k} = 0, \tag{15d}$$

$$\frac{\partial \Sigma_{ik}}{\partial t} - \mu\left(\left(\frac{\partial V^i}{\partial x_k} + \frac{\partial V^k}{\partial x_i}\right) - \frac{2}{3}\delta_{ik}\left(\frac{\partial V^1}{\partial x_1} + \frac{\partial V^2}{\partial x_2} + \frac{\partial V^3}{\partial x_3}\right)\right) = -\frac{\Sigma_{ik}}{\tau}, \tag{15e}$$

Here, $c_a^0 = \alpha_a^0 \rho_a^0 / \rho_0, (a = 1, 2)$, $\rho_0 = \alpha_1^0\rho_1^0 + \alpha_2^0\rho_2^0 + \alpha_3^0\rho_3^0$, $K = \left(\frac{\alpha_1^0}{K_1} + \frac{\alpha_2^0}{K_2} + \frac{\alpha_3^0}{K_3}\right)^{-1}$ is the bulk modulus of the mixture and $K_a' = (\alpha_a^0 - c_a^0)K$, $a = 1, 2$. The friction source terms Λ_a^i can be rewritten in terms of W_a^i as

$$\Lambda_1^i = \lambda_{11}' W_1^i + \lambda_{12}' W_2^i, \qquad \Lambda_2^i = \lambda_{21}' W_1^i + \lambda_{22}' W_2^i, \tag{16a}$$

$$\begin{pmatrix} \lambda_{11}' & \lambda_{12}' \\ \lambda_{21}' & \lambda_{22}' \end{pmatrix} = \begin{pmatrix} \lambda_{11} & \lambda_{12} \\ \lambda_{21} & \lambda_{22} \end{pmatrix} \begin{pmatrix} -(1-c_1^0)c_1^0 & c_1^0 c_2^0 \\ c_1^0 c_2^0 & -(1-c_2^0)c_2^0 \end{pmatrix}. \tag{16b}$$

In the subsequent analysis of wave propagation and numerical examples we assume that both fluids are ideal $c_{s,1}^2 = c_{s,2}^2 = 0$ and solid skeleton is pure elastic. Therefore we take $\tau = \infty$ and $\mu = \rho c_{s,M}^2 = \rho c_3^0 c_{s,3}^2 = \alpha_3^0 \mu_3$, where μ, μ_3 are the shear moduli of the mixture and of the solid phase.

4 Dispersion Relations

In this section we study the dependence of one-dimensional longitudinal waves on their frequency. The dispersion relation $k(\omega)$ for the linear equations (15) can be computed exactly in the same way as in our previous work [7]. Here, k is the complex wavenumber and ω is the real angular frequency. Figure 1 shows phase velocities of the fast $V_{\text{fast}}(\omega)$ and slow $V_{\text{slow}}(\omega)$ compressional waves as a function of angular frequency $\omega = 2\pi f$ (f is the standard frequency) for the porosity $\phi = 0.3 = 1 - \alpha_3^0$ and several values of the volume fraction of gaseous phase: $\alpha_2^0 = 10^{-2}$, 10^{-3}, 10^{-4}, 10^{-5}, and 0. To plot this figure, we set $\lambda_{12}' = \lambda_{21}' = 0$ and took $\lambda_{11}' = 10^3 \sim \eta_{water}^{-1}$ and $\lambda_{22}' = 54 \cdot 10^3 \sim \eta_{air}^{-1}$, where η_{water} and η_{air} are the water and air viscosities. To plot all curves in a single plot, the phase

velocities were normalized by the characteristic velocities (eigenvalues of the left hand-side of simplified one-dimensional version of (15)) which are given by

$$C^2_{\text{fast,slow}} = \frac{K + \frac{4}{3}\mu + Z \pm \sqrt{-\frac{16}{3}\mu Z + \left(K + \frac{4}{3}\mu + Z\right)^2}}{2\rho} \tag{17a}$$

$$Z = \rho\left(R_1 K_1' + R_2 K_2'\right), \qquad R_a = \frac{1}{\rho_a^0} - \frac{1}{\rho_3^0}, \quad a = 1, 2. \tag{17b}$$

and are equal to $C_{\text{fast}} = 4039$ m/s and $C_{\text{slow}} = 331$ m/s for $\alpha_2^0 = 10^{-2}$, $C_{\text{fast}} = 4037$ m/s and $C_{\text{slow}} = 342.3$ m/s for $\alpha_2^0 = 10^{-3}$, $C_{\text{fast}} = 4096$ m/s and $C_{\text{slow}} = 422.8$ m/s for $\alpha_2^0 = 10^{-4}$, $C_{\text{fast}} = 4301$ m/s and $C_{\text{slow}} = 607.1$ m/s for $\alpha_2^0 = 10^{-5}$, and $C_{\text{fast}} = 4441$ m/s and $C_{\text{slow}} = 692.9$ m/s for $\alpha_2^0 = 0$.

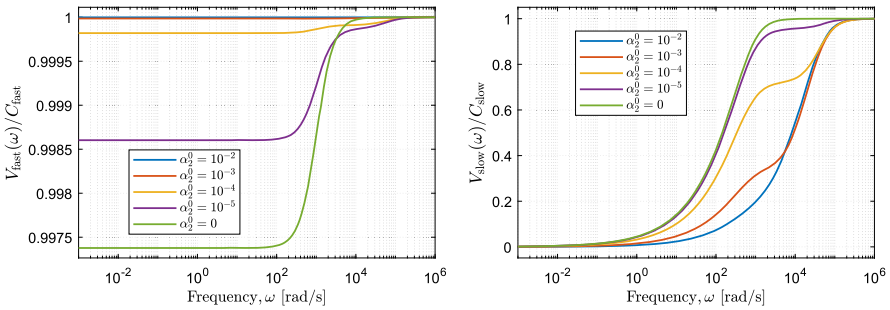

Fig. 1. Normalized phase velocities of the fast and slow compressional waves for various volume fractions of the gaseous phase.

5 Numerical Simulations

In this section we numerically illustrate the main features of small amplitude wavefields described by system (15). For simulations, we use finite difference schemes on staggered grids [12,13]. This approach is most suitable for solving first order symmetric hyperbolic systems in the velocity-stress formulation. By analogy to the Levander approach [8,13], we developed a fourth-order accurate scheme on a staggered grid in space and a second-order accurate scheme in time for modeling the wave propagation in a porous medium saturated with a two-fluid compressible mixture.

We consider a homogeneous porous medium saturated with a mixture of two fluids. Let us call the liquid phase Fluid1, the gas phase Fluid2 and the skeleton Solid with material parameters from Table 1.

The goal of solving the first series of test problems, in some of which a homogeneous medium is defined as one pure phase out of three, is to validate the model. Let us consider four cases: pure Solid ($\alpha_1^0 = \alpha_2^0 = 0, \alpha_3^0 = 1$), pure Fluid1 ($\alpha_1^0 = 1, \alpha_2^0 = \alpha_3^0 = 0$), pure Fluid2 ($\alpha_1^0 = \alpha_3^0 = 0, \alpha_2^0 = 1$),and poroelastic case with Solid and only one Fluid1 ($\alpha_1^0 = 0.3, \alpha_2^0 = 0, \alpha_3^0 = 0.7$).

The computational domain is discretized with $N_x \times N_y$ grid points, $N_x = N_y = 2001$ with spatial step $d_x = d_y = 2.5 \cdot 10^{-5}\ m$, which amounts to approximately 13 points per a slow compressional wavelength for a chosen frequency $f_0 = 1$ MHz.

To excite the volumetric-type source we add a source term in the right-hand side of the pressure equation of the system (15). A source function is defined as the product of Dirac's delta function in space and Ricker's wavelet $f(t)$ in time:

$$f(t) = (1 - 2\pi^2 f_0^2 (t - t_0)^2) exp[-\pi^2 f_0^2 (t - t_0)^2], \tag{18}$$

where f_0 is the source central frequency and t_0 is the time wavelet delay. We assumed the frequency $f_0 = 1$ MHz and the source time delay $t_0 = 1/f_0$ s. The source is located in the centre of the computational domain.

Figure 2 shows the wavefield snapshots of the norm of the total mixture velocity vector $\| V \|^2$ at time $t = 4 \cdot 10^{-6}\ s$ for four cases. As one can expect, the velocities of arising waves coincide with P-wave velocity for pure Solid ($v_p = 6155\ m/s$) and sound velocities c_{f1}, c_{f2} for pure Fluid1 ($c_{f1} = 1500\ m/s$) and Fluid2 ($c_{f2} = 330\ m/s$) from Table 1. Only one compressional P-wave arises in the case of pure solid, pure water or pure gas (Fig. 2a–2c). In the case of poroelasticity, we can observe the appearance of fast and slow (Biot's mode) compressional waves (Fig. 2d). Estimated velocities 4440 m/s for the fast wave and 690 m/s for the slow wave are well consistent with the velocity dispersion curves in Fig. 1, obtained with the technique described in [7]. When evaluating the velocities, one should keep in mind Ricker's wavelet delay of $1 \cdot 10^{-6}\ s$ for chosen poroelastic model with Solid and Fluid1 parameters from Table 1 and porosity $\alpha_1^0 = 0.3$.

Table 1. Physical parameters used for simulation.

State	Property	Parameters	Value	Unit
Fluid1 (water):	Fluid density	$\rho_{f1} = \rho_1^0$	1040	kg/m^3
	Sound velocity	c_{f1}	1500	m/s
	Bulk modulus	$K_{f1} = K_1 = \rho_{f1} c_{f1}^2$	2.34	GPa
Fluid2 (air):	Fluid density	$\rho_{f2} = \rho_2^0$	1.225	kg/m^3
	Sound velocity	c_{f2}	330	m/s
	Bulk modulus	$K_{f2} = K_2 = \rho_{f2} c_{f2}^2$	0.13	GPa
Solid:	Solid density	$\rho_s = \rho_3^0$	2500	kg/m^3
	P-wave velocity	v_p	6155	m/s
	Bulk velocity	c_s	4332	m/s
	Shear velocity	c_{sh}	3787	m/s
	Bulk modulus	$K_s = K_3 = \rho_s c_s^2$	46.91	GPa
	Shear modulus	$\mu_s = \mu_3 = \rho_s c_{sh}^2$	35.85	GPa

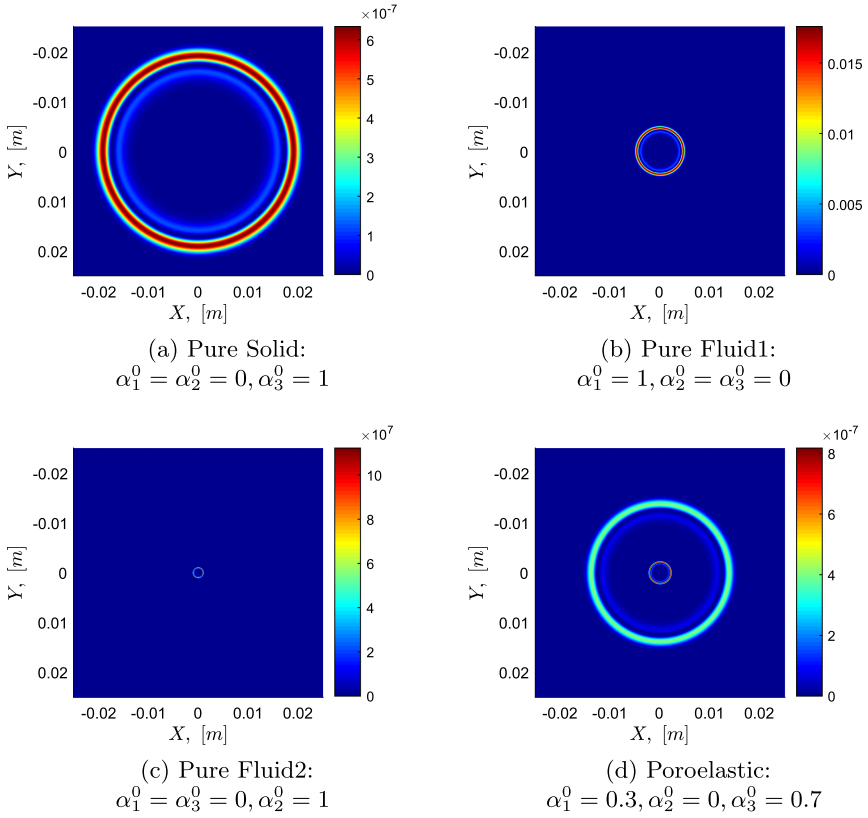

(a) Pure Solid: $\alpha_1^0 = \alpha_2^0 = 0, \alpha_3^0 = 1$

(b) Pure Fluid1: $\alpha_1^0 = 1, \alpha_2^0 = \alpha_3^0 = 0$

(c) Pure Fluid2: $\alpha_1^0 = \alpha_3^0 = 0, \alpha_2^0 = 1$

(d) Poroelastic: $\alpha_1^0 = 0.3, \alpha_2^0 = 0, \alpha_3^0 = 0.7$

Fig. 2. Wavefield snapshots of $||V||^2$ for pure Solid (a), pure Fluid1 (b), pure Fluid2 (c) and poroelastic (d) media at time $t = 4 \cdot 10^{-6}$ s.

The second test investigates the effect of gas presence on the wave propagation velocity in a three-phase poroelastic medium. To this end, let us vary the value of volume fraction α_2^0 of the air (Fluid2), while the Solid volume fraction being constant $\alpha_3^0 = 0.7$ and porosity is $\alpha_1^0 + \alpha_2^0 = 0.3$. With this consideration, the sample's porosity remains constant, only the ratio of Fluid1 and Fluid2 changes.

Figure 3 shows the wavefield snapshots of the total mixture velocity vector $\| V \|^2$ for poroelastic media with porosity $\alpha_1^0 = 0.299, \alpha_2^0 = 0.001, \alpha_3^0 = 0.7$ at time $t = 4 \cdot 10^{-6}$ s. Comparing phase velocities in the case of two different ratios of liquid and gas volume fractions with $\alpha_1^0 = 0.3, \alpha_2^0 = 0, \alpha_3^0 = 0.7$ and $\alpha_1^0 = 0.299, \alpha_2^0 = 0.001, \alpha_3^0 = 0.7$, one can notice that the velocity of the fast P

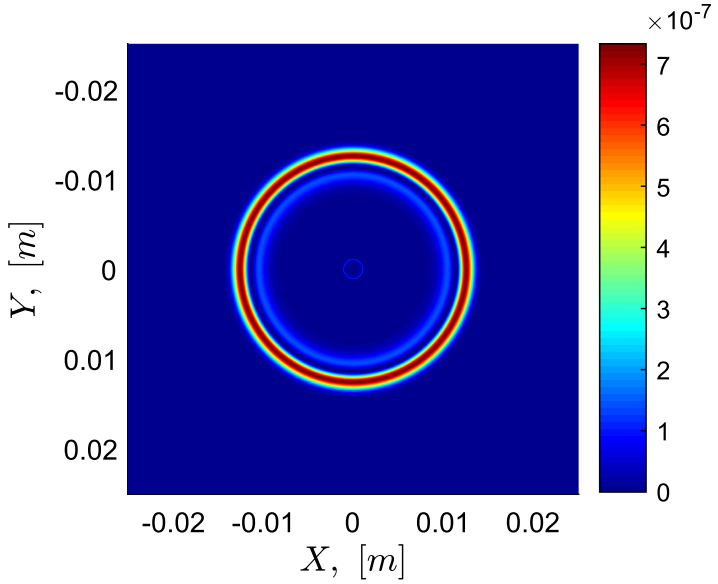

Fig. 3. Wavefield snapshot of $||V||^2$ for poroelastic medium with phase volume fractions $\alpha_1^0 = 0.299, \alpha_2^0 = 0.001, \alpha_3^0 = 0.7$ at time $t = 4 \cdot 10^{-6}$ s.

wave has decreased slightly, while the velocity of the Biot mode has decreased by almost half. That is more, the amplitude of the Biot mode has decreased significantly in comparison with Fig. 2d. In order to trace the dependence on the gas volume fraction α_2^0, we compared snapshot slices of V^1 component passing vertically through $x = 0$ for different parameters $\alpha_2^0 = 0, 0.001, 0.005, 0.01$ and plotted them together in Fig. 4. From a comparison of these cases, the following conclusions can be drawn. With an increase in the parameter α_2^0, the velocity of the fast and slow compressional P waves decreases. Simultaneously, the fast P wave amplitude increases, while the amplitude of Biot's mode decreases very fast with a small increase in α_2^0.

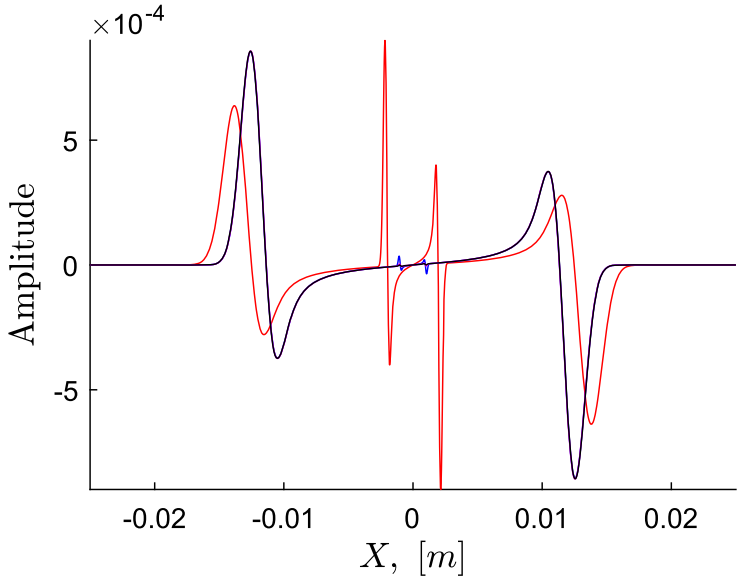

(a)

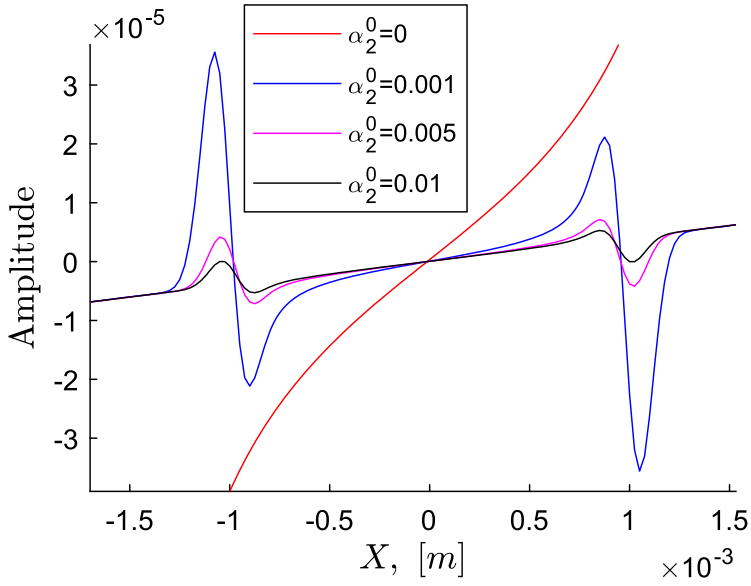

(b) zoom near $x = 0$

Fig. 4. Snapshot slices of V^1 component at time $t = 4 \cdot 10^{-6}$ s passing through $x = 0$ for different parameters $\alpha_2^0 = 0, 0.001, 0.005, 0.01$.

6 Conclusions

We have presented a new computational model of a deformed porous medium saturated with a compressible mixture of two fluids. The governing equations of the model are hyperbolic and are consistent with two thermodynamic laws: conservation of energy and growth of entropy. A simplified computational model for the propagation of small-amplitude waves is formulated and some test problems are solved numerically using the finite difference method on staggered grids. The applicability of the model is shown for studying the features of wavefields in an elastic porous medium saturated with liquid and gas, including the dependence of wave velocities and amplitudes on their ratio.

References

1. Biot, M.A.: Theory of propagation of elastic waves in fluid-saturated porous solid. I. Low-frequency range. J. Acoust. Soc. Am. **28**(2), 168–178 (1956)
2. Biot, M.A.: Theory of propagation of elastic waves in a fluid-saturated porous solid. II. Higher frequency range. J. Acoust. Soc. Am. **28**(2), 179–191 (1956)
3. Carcione, J.M., Morency, C., Santos, V.: Computational poroelasticity - a review. Geophysics **75**(5), 75A229–75A243 (2010)
4. Pesavento, F., Schrefler, B.A., Sciumè, G.: Multiphase flow in deforming porous media: a review. Arch. Comput. Methods Eng. **24**(2), 423–448 (2016). https://doi.org/10.1007/s11831-016-9171-6
5. Wilmanski, K.: A thermodynamic model of compressible porous materials with the balance equation of porosity. Transp. Porous Media **32**(1), 21–47 (1998)
6. Wilmanski, K.: A few remarks on Biot's model and linear acoustics of poroelastic saturated materials. Soil Dyn. Earthq. Eng. **26**(6–7), 509–536 (2006)
7. Romenski, E., Reshetova, G., Peshkov, I., Dumbser, M.: Modeling wavefields in saturated elastic porous media based on thermodynamically compatible system theory for two-phase solid-fluid mixtures. Comput. Fluids **206**, 104587 (2020)
8. Reshetova, G., Romenski, E.: Diffuse interface approach to modeling wavefields in a saturated porous medium. Appl. Math. Comput. **398**(C), 125978 (2021)
9. Dumbser, M., Peshkov, I., Romenski, E., Zanotti, O.: High order ADER schemes for a unified first order hyperbolic formulation of continuum mechanics: viscous heat-conducting fluids and elastic solids. J. Comput. Phys. **314**, 824–862 (2016)
10. Dumbser, M., Peshkov, I., Romenski, E., Zanotti, O.: High order ADER schemes for a unified first order hyperbolic formulation of Newtonian continuum mechanics coupled with electro-dynamics. J. Comput. Phys. **348**, 298–342 (2017)
11. Romenski, E., Belozerov, A., Peshkov, I.M.: Conservative formulation for compressible multiphase flows. Q. Appl. Math. **74**(1), 113–136 (2016)
12. Virieux, J.: P-SV wave propagation in heterogeneous media: velocity-stress finite-difference method. Geophysics **51**(1), 889–901 (1986)
13. Levander, A.R.: Fourth-order finite-difference P-W seismograms. Geophysics **53**(11), 1425–1436 (1988)